Colloid Polym Sci 279:166–170 (2001)

SHORT COMMUNICATION

H. J. Vogel
G. Baur
W. Burchard

Quantitative determination of large structures by small-angle light scattering

Received: 06 December 1999
Accepted: 04 February 2000

H. J. Vogel · G. Baur · W. Burchard
Institute of Macromolecular Chemistry
University of Freiburg
79104 Freiburg Germany

Abstract A new small-angle light scattering camera has been developed. In contrast to conventional detection the present system is based on a recently developed two-dimensional charge-coupled-device chip made by Thomson (France). The advantage of this chip is its excellent linear response and very low dark signal even at room temperature. The best linearity was obtained by leading each pixel signal through the same amplifying system. The optical system covered a diffraction angular region from about 1° to 15° ($q = 0.2$–$2.6\ \mu m^{-1}$). The camera was calibrated with grids and pinholes and was tested with polymer latex particles in solution and with spherulites from polymer films.

Key words Small-angle light scattering · Absolute scattering intensity detection · Large particles · Semi-dilute solutions · Scattering from grids

Introduction

Common static wide-angle light scattering (WALS) is a well-established technique in polymer science for determination of the molar mass (M_w) and the radius of gyration (R_g) of individual macromolecules in dilute solution. However, the dimensions of these molecules can be measured for samples with $R_g > 12$ nm, which often corresponds to molar masses of $M_w > 10^5$ g/mol. For the determination of nanostructures much shorter wavelengths have to be used, for example, X-rays or cold neutrons. The wavelengths of these sources are at least 1000 times shorter than those of visible light. This requires the highly developed techniques of small-angle X-ray scattering (SAXS) and small-angle neutron scattering (SANS) for structure investigations of oligomers and polymers in the region down to $M_w \approx 1000$ g/mol.

Recently, there has been much interest in the preparation of supramolecular structures and their characterization. Such supramolecular structures, composed of macromolecules, often exhibit dimensions of the order of microns. Heterogeneities of similar size also occur in thermoreversible gel formation [1]. Another subject of interest is structure formation on phase separation. Here again very large heterogeneities are formed before macroscopic phase separation takes place.

In all these cases neither WALS nor the present techniques of SAXS or SANS are able to detect such large structures. Much effort has been invested in further extending the SANS region to even lower values of $q = (4\pi/\lambda)\sin(\theta/2)$, which has led to ultra-small-angle neutron scattering. Very promising results have been reported recently [2]. Here, we follow an alternative route and extend WALS measurements to the small-angle light scattering region (SALS) and simultaneously to a registration in two dimensions. This is achieved by employing a charge-coupled-device (CCD) chip as a two-dimensional multichannel detector. The technique of SALS is not really new. Quite a few experiments have already been carried out [3–19] and theoretical work has also been reported [20–28]. However, in previous studies most of the experiments remained confined to the registration of qualitative behavior [3–10]. This restriction was based on the use of photographic techniques or photodetection devices [6–10], which did not permit undistorted detection of scattering intensities. The quality of those instruments could be considered as adequate, because mostly semicrystalline samples were

studied in the past. Here, the exact position of the angles is important, but exact angular envelopes are not essential. Only a few attempts to measure quantitatively the scattered intensities are found in the literature [11–18]. Recently, a SALS camera was reported that can be used even for dynamic light scattering measurements [19] and that is quite similar to our construction.

Our interest is focussed on semidilute and concentrated solutions [29], where much lower scattering intensities have to be determined quantitatively. Because of the recent production of an improved generation of CCD chips, detection of absolute intensities can be performed correctly. In the first part of a series we report details of the construction of a SALS camera and some test measurements with geometric and well-defined colloidal samples.

SALS camera

CCD chip

The heart of the SALS camera consists of the TH 7895M-(L) CCD chip (Thomson, France). This device is a full-field CCD image sensor optimized for a wavelength range of 400–1100 nm and delivers 512×512 data pixel points with an effective aperture of 19×19 μm each. The striking advantage of this chip is its excellent linear response and its very low dark signal, even at room temperature. A high signal-to-noise ratio for the measured light intensity is obtained without cooling the chip. Thus, a maximum data depth up to 16 bit (cooled 18 bit) is possible. To reach similar behavior with common chips, cooling temperatures of −40 to −80 °C have to be applied, which intriguingly cause high-temperature gradients, in particular when the sample is to be heated.

Electronics

For the data management special fast, yet still reliable, read-out electronics had to be designed. The present development allowed the use of the SALS camera in combination with a common personal computer. The shortest applicable exposure time is about 15 ms and depends mainly on the self-made shutter mechanics. The fairly long read-out time of about 3 s is due to the chosen serial technique, which is required for linear response. The data pixels on the chip are organized in rows. The read-out is performed by serial transfer of the information from one specific row (last). After that all other rows are shifted synchronously by one row and are again read out, etc. The advantage of the electronic simplicity is the high accuracy of data processing (the same amplification for each pixel). Its disadvantage is the already mentioned fairly long read-out time of 3 s. Also the long read-out time causes some additional exposure, for example, from dark current and weak stray light.

Further fluctuations in accuracy result from differences in the response quality of the individual pixels and from the dark current. These imperfections are partially removed when the scattering intensities of the solvent measurements are subtracted. Low-cost CCD chips make use of common frame-transfer techniques which avoid additional exposures, but this deteriorates the information quality from the pixels. The charge-transfer efficiency (CTE) for common chips is about 0.9999, whereas for the TH7895M-(L) chip the CTE of 0.999998 is 50 times better and is combined with a very low dark current.

Optics

As a light source a 1122P polarized 2-mW HeNe laser from Uniphase (Eching, Germany) was used. The wavelength was 632.8 nm and the degree of polarization was designated as 500:1. The optical setup of the camera is shown in Fig. 1. An optimized optical path was calculated using Gaussian optical methods for paraxial rays combined with matrix methods [30]. The results were confirmed with the aid of the computer program WINLENS from Spindler & Hoyer (Göttingen, Germany).

To minimize the scattering volume, lens L1 slightly focuses the primary beam of the laser light. The beam develops a divergence of about 3 mrad in the focus region around the sample position. The primary beam is monitored by a scatter-glass that emits a small part of the primary beam onto a photodiode. By a voltage–frequency converter the light intensity is transformed into a pulse sequence. This sequence can be used to monitor the total amount of light. With this device fluctuations in the laser intensity are largely eliminated. The device also controls the shutter and guarantees that exactly the same amount of light is available for each measurement in a series of measurements. Two lenses and a pinhole, representing a space filter, are positioned in the optical path, which removes optical diffraction patterns from the source and the preceding optics. The

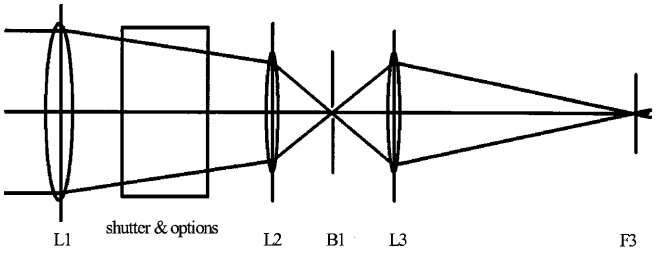

Fig. 1 Optical setup of the small-angle light scattering camera. The extreme rays through the prefocusing lens *L1*, the shutter and options box and the space filter (*L2*, *B1*, *L3*) are shown. The sample is positioned in the focus plain *F3*. The scattering pattern is imaged via lens *L4* onto the charge-coupled-device chip (not shown)

scattered rays are imaged by a Fourier lens onto the CCD chip surface. This design promises best results for scattering patterns on minimized aberrations and other errors. Between the sample cell and the Fourier lens a polarization analyzer can be inserted. With this option the optical anisotropy of the sample can be determined with both polarizers vertical or with crossed polarizers. Immediately in front of the CCD chip an IR filter is placed to reduce the amount of thermal radiation hitting the CCD surface. This filter also improves errors from stray light, in particular when the sample is heated to elevated temperatures.

Sample holder and cell

The construction of the sample holder enables precise positioning of flat sample cells or sliced materials. Liquids as well as thin films or other transparent solid pieces can be measured in a temperature range from 0 to 150 °C. For a liquid specimen a special flat glass cell was designed, which can be inserted into the sample holder.

Data management

For data management special adapted computer programs were developed. Simple picture viewing, data collecting, averaging mechanisms and data simulation procedures are possible. The two-dimensional pictures (512×512 pixels) were stored in compressed files and can be converted and exported to common BIDMAP format files. Cross sections or averaged data were exported into ASCII files.

Test measurements

Calibration of the SALS camera was made by scattering patterns from geometric samples, where the diffraction patterns are theoretically well known. The geometric samples consist of optical precision grids, $g = 100$, and a set of pinholes with diameters from 50 to 400 μm. The two items can be used to detect and correct errors concerning the position of scattering angles and the linearity in the intensity amplifying system, respectively. The calibrations were followed by some tests with colloidal systems and polymer films containing semicrystalline spherulites.

Geometric samples

1 Grid

For testing the exact function of the CCD camera diffraction experiments with well-defined geometric samples were required. The correctness of the pixel-to-angle correlation was checked using a precision optical grid (Newport, Darmstadt) with a grid constant of $g = 100$ μm. The theoretical scattering pattern from this grid is given [31] by the equation

$$I_s = I_0 \frac{\sin^2\left(\frac{\pi p g}{\lambda}\sin\theta_x\right)\sin^2\left(\frac{\pi b}{\lambda}\sin\theta_x\right)\sin^2\left(\frac{\pi h}{\lambda}\sin\theta_y\right)}{\sin^2\left(\frac{\pi g}{\lambda}\sin\theta_x\right)\left(\frac{\pi b}{\lambda}\sin\theta_x\right)^2\left(\frac{\pi h}{\lambda}\sin\theta_y\right)^2} \quad . \quad (1)$$

Here g is the grid constant, p the number of illuminated grid elements, b is the breadth and h is the height of one groove. θ_x and θ_y are the detecting angles and λ is the wavelength of the laser light (Fig. 2).

The experimental data are compared with the theoretical predictions in Fig. 3. It was possible to correct the diffraction pattern for first-order aberration caused by the Fourier lens. At the largest angles some weak errors of higher order could still be left, but they are below the detection accuracy.

2 Pinholes

The linearity of intensity amplification was tested with pinholes. The experimental data were compared with the

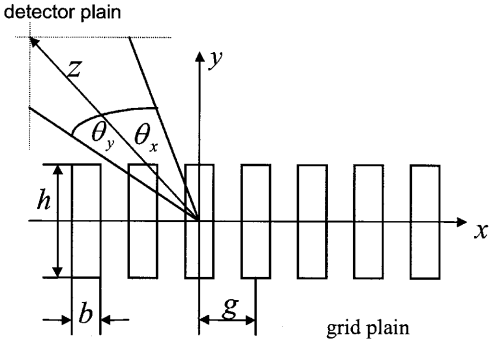

Fig. 2 Diffraction pattern from a grid

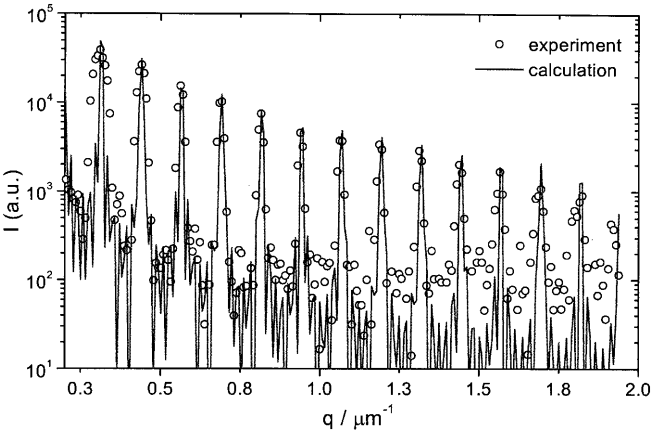

Fig. 3 Diffraction pattern and simulation of an optical precision grid with $g = 100$ μm

theoretical diffraction pattern [31] that is given by the Airy function

$$I(q) \propto \frac{J_1(Rq)}{Rq} \quad , \tag{2}$$

where $J_1(x)$ is the first-order Bessel function and R is the radius of the pinhole. The result of the experiment in comparison to theory is shown in Fig. 4.

Colloidal samples

1 Polymer latices

Polymer latex beads are suitable polymer test samples for SALS experiments because of their spherical shape and large size. However, problems arose in finding samples of proper narrow size distribution and concentration. The best results were expected with polystyrene divinylbenzene latex beads of (6.4 ± 2.0)-μm diameter (Sigma-Aldrich, Steinheim, Germany). Unfortunately, the high-order intensity maxima were hardly detectable because of a broad size distribution of about 30%. The experimental scattering patterns of a dilute dispersion and the theoretical prediction are shown in Fig. 5. The prediction refers to Rayleigh scattering from a sphere of (6.56 ± 0.02)-μm diameter combined with particles of any shape of (8.22 ± 0.06)-μm diameter. This combination corresponds to the size distribution and the fact that the measured diameters are z averages as is common in light scattering. It should be mentioned that Rayleigh's approximation fails for large spheres of high optical refraction ratio ($m \gg 1$) with respect to the surroundings. For polystyrene spheres in water m is about 1.26, yielding $am \approx 4$, where a is the latex radius.

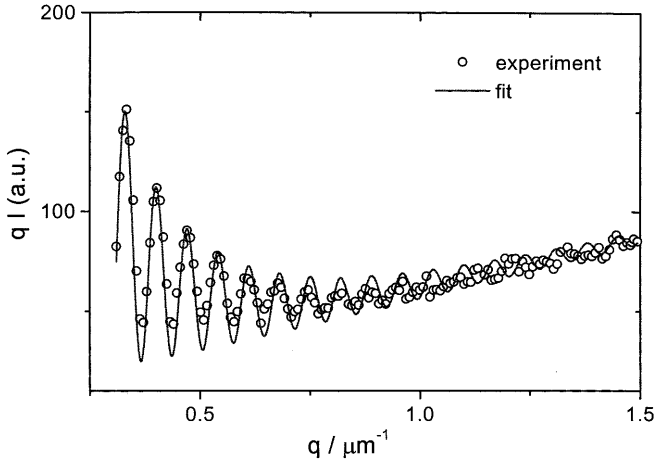

Fig. 4 Plot of measured scattering intensities versus scattering vector of the diffraction pattern from an optical pinhole of 90-μm in diameter compared with the theoretically expected behavior (see Eq. 2)

Rayleigh's approximation was still employed instead of the exact but rather complex equations derived by Mie [20].

2 Spherulites

The polarization facilities of the SALS camera were tested by scattering from some semicrystalline polymeric spherulites. As an example, a film of syndiotactic polystyrene spherulites of known size was measured under crossed polarization. The scattering patterns of ideal spherulites of known radii can be calculated with equations derived by Stein and Rhodes [22]. The calculated pattern was compared with experimental results and is shown in Fig. 6. The radii of the spherulites were checked by optical microscopy. The differences between calculation and experiment can again be explained by a wide size distribution of the

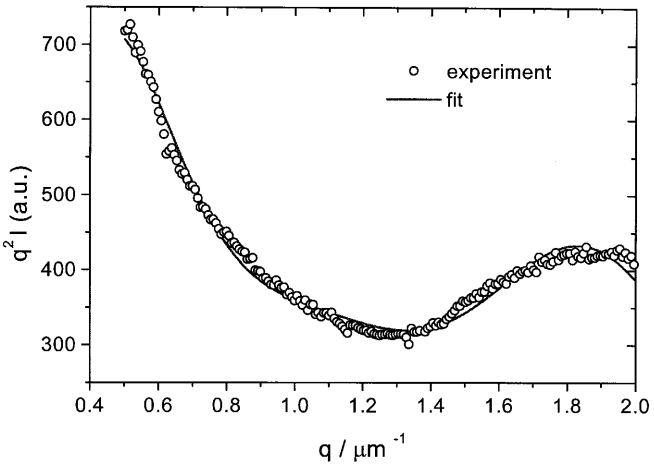

Fig. 5 Scattering and fitted curves from polymer latices (*L6*). The fit was made by a Guinier approximation for the low-angle region (resulting in a radius of $R_1 = 4.11 \pm 0.03$ μm) and with the particle scattering factor of monodisperse spheres with $R_2 = 3.28 \pm 0.01$ μm

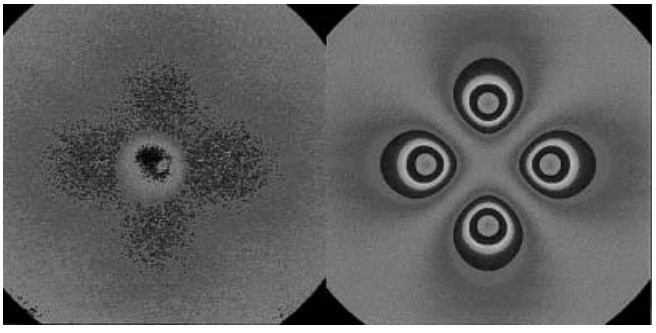

Fig. 6 Depolarized scattering pattern from spherulites. *Left*: experiment; *right*: calculate

spherulites. A good fit was obtained when a bimodal size distribution was assumed.

Discussion

A two-dimensional CCD camera has been developed to detect simultaneously SALS in an angular range from about 1° to 15°. Employing a new special CCD chip permitted a very high signal-to-noise ratio even at room temperature. This restricts undesired temperature gradients under heating conditions. In order to receive optimum linear amplified signals for each CCD pixel special data-read-out electronics were designed. The optical setup was optimized to receive a filtered and well-controlled parallel laser beam through the sample cell after the scattering light has been focussed onto the CCD chip. The camera is fully controlled by a personal computer (i.e. Pentium III) and the scattering images can be analyzed using self-written software. The maximum achievable data size of one data pixel is 16 bit under uncooled conditions (18 bit when the CCD chip is cooled to −40 °C), but stray light and thermal noise can reduce the usable data range significantly. The camera was calibrated with optical precision grids with grid constants of $g = 100$ and a set of pinholes with diameters from 50 to 400 μm. The calibration was confirmed with test measurements of polymer latex beads of different diameters from about 1 to 12 μm and with polymer films consisting of semicrystalline spherulite structures. The results of the test measurements confirm that the CCD camera delivers correct data under convenient conditions. Some problems remained, for example, ''blooming'' effects at high exposure times, stray light and thermal noise. Most of these problems can be managed or will be removed in future.

We mentioned already the SALS camera constructed by Cipelletti and Weitz [19] that has a very similar setup compared to ours. The authors were interested in the observation of very slow dynamic processes occurring with aging of colloidal systems. They studied these processes by measuring the time correlation function of speckle scattering. The scattering intensities were circular by averaged for various image radii, and the time correlation function was formed by a personal computer for each ring in the normal manner. Our interest, so far, has been focussed on the detection of static structure factors; however, the camera can also be used for the detection of slow motions.

Acknowledgement The work was financially supported by the Deutsche Forschungsgemeinschaft within the special research scheme Cellulose and Cellulose Derivatives.

References

1. (a) Burchard W, Aberle T, Fuchs T, Richtering W, Coviello T, Geissler E, Schulz L (1998) Polym Networks Group Ser 1:2; (b) Coviello T, Burczard W, Geissler E, Maier D (1997) Macromolecules 30:2008; (c) Bastide J, Leibler L, Prost J (1990) Macro molecules 23:1821
2. (a) Kroupa G, Bruckner G, Baron M, Villa M, Hainbuchner M, Rauch H (2000) J. Appl. Cryst. 33: 851; (b) Hagenmayer RM, Zeyen CME, Lamparter P, Steeb S (1993) Z Naturforsch A Phys Sci 48:1203; (c) Kanaya T, Takeshita H, Nishikoji Y, Ohkura M, Nishida K, Kaji K (1998) Supramol Sci 5:215; (d) Agmalian M, Alamo RG, Kim MH, Londono JD, Mandelkern L, Wignall GD (1999) Macromolecules 32:3093
3. Stein RS, Wilkes GL (1975) In: Ward IM (ed) structure and properties of oriented polymers. Applied Science, London, Chapt. 3, pp 57
4. Stein RS, Srinivasarao M (1993) J Polym Sci B 31:2003
5. Mallamace F, Micali N (1996) In: Brown W (ed) Light scattering, principles and development. Clarendon, Oxford, Chapt. 12, pp 381
6. Qu BJ, Ranby B (1993) J Appl Polym Sci 49:1799
7. Li Y, Liu J, Yang H, Ma D, Chu B (1993) J Polym Sci B 31:853
8. Cheung YW, Stein RS, Lin JS, Wignall GD (1994) Macromolecules 27:2520
9. Kwak SY (1995) J Appl Polym Sci 55:1683
10. van Egmond JW, Werner DE, Fuller GG (1992) J Chem Phys 96:7743
11. Carpineti M, Ferri F, Giglio M, Paganini E, Perini U (1990) Phys Rev A 42:7347
12. Okada T, Saito H, Inoue T (1992) Macromolecules 25:1908
13. Cumming A, Wiltzius P, Bates FS, Rosedale JH (1992) Phys Rev E 45:885
14. Lauger J, Gronski W (1995) Rheol Acta 34:70
15. Kume T, Asakawa K, Mose E, Matsuzaka K, Hashimoto T (1995) Acta Polym 46:79
16. Tromp RH, Rennie AR, Jones RAL (1995) Macromolecules 28:4129
17. Murthy NS, Zero K, Grubb DT (1997) Polymer 38:1021
18. Ferri F (1997) Rev Sci Instrum 68:2265
19. Cipelletti L, Weitz DA (1999) Rev Sci Instrum 70:3214
20. Mie G (1909) Ann Phys 25:377
21. Guinier A, Fournet G (1955) Small angle scattering of X-rays. Wiley, New York
22. Stein RS, Rhodes MB (1960) J Appl Phys 31:1873
23. Samuels RJ (1971) J Polym Sci A-2 9:2165
24. Hashimoto T, Nakai A, Shiwaku T, Hasegawa H, Rojstaczer S, Stein RS (1989) Macromolecules 22:422
25. Meeten GH (1989) J Polym Sci Part B Polym Phys 27:2023
26. Svergun DI (1991) J Appl Crystallogr 24:485
27. Holoubek J (1994) J Polym Sci Part B Polym Phys 32:351
28. Ofoli RY, Prieve DC (1997) Langmuir 13:4837
29. (a) Galinsky G, Burchard W (1996) Macromolecules 29:1498; (b) Aberle T, Burchard W (1999) In: Colonna P, Guilbert S (eds) Biopolymer science: food & non-food applications. INRA, Paris, Vol. 91, pp 247; (c) Aberle T, Burchard W (1997) Comput Theor Polym Sci 7:215; (d) Aberle T, Burchard W (1997) Starch 49:215
30. Brouwer W (1964) Matrix methods in optical instrument design. Benjamin, New York
31. Born M (1965) Optik 2nd edn. Springer, Berlin Heidelberg New York